Identification of ^{129}I interferences in accelerator mass spectrometry

Sheng Xu*, Stewart P.H.T. Freeman

Scottish Universities Environmental Research Centre (SUERC)

East Kilbride, G75 0QF, U.K.

*Corresponding author: sheng.xu@glasgow.ac.uk

Abstract

The identification of interferences to $^{129}I^{n+}$ (n = 3-6) was conducted with a 5 MV tandem accelerator mass spectrometer at SUERC. In addition to ^{128}Te, the detectable interferences to 12 MeV $^{129}I^{3+}$ ions include $^{43}Ca^{1+}$ and $^{86}Sr^{2+}$ which are likely injected as $^{43}Ca^{86}Sr^{-}$, $^{43}Ca^{32}S^{18}O_3^{-}$, etc. whereas those to 15 MeV $^{129}I^{4+}$ ions include $^{32}S^{1+}$ injected as $^{43}Ca^{32}S^{18}O_3^{-}$, $^{65}Cu^{2+}$ as $^{63}Cu^{65}Cu^{1}H^{-}$, $^{97}Mo^{3+}$ as $^{97}Mo^{16}O_2^{-}$. The 18 MeV $^{129}I^{5+}$ ions might be interfered by $^{77}Se^{3+}$ and $^{104}Pd^{4+}$ (or $^{104}Ru^{4+}$) and the 21 MeV $^{129}I^{6+}$ ions by $^{43}Ca^{2+}$, $^{65}Cu^{3+}$, $^{86}Sr^{4+}$ and $^{108}Pd^{5+}$ (or $^{107}Ag^{5+}$, $^{108}Cd^{5+}$). Apart from ^{128}Te, these ions can be fully separated from ^{129}I in the gas ionization detector equipped with a thin SiN membrane window and propane gas, which contributes negligibly to the ^{129}I-AMS detection for samples after careful chemical preparation. Although the ^{129}I background is mainly controlled by Te content and the source memory, the rareness of Te in natural environmental samples results in our routine background $^{129}I/^{127}I$ level in range of ~10^{-14}. The precision and accuracy of 3 % can be routinely achieved at $^{129}I/^{127}I > 10^{-12}$ level at SUERC.

Keywords: ^{129}I, interference, molecular fragment, accelerator mass spectrometer

1. Introduction

Iodine-129 (^{129}I; $t_{1/2} = 1.57 \times 10^7$ year) is one of the most important cosmogenic radionuclides generated in the Earth's atmosphere. It is also one of the most important fissiongenic nuclides of uranium produced naturally in terrestrial rocks and authropogenically from nuclear activities (e.g., nuclear weapon tests, nuclear power generation, spent fuel reprocessing, etc.). In particular, the authropogenic ^{129}I released from the spent fuel reprocessing plants since the 1950-60's has resulted in the abrupt increase of environmental $^{129}I/^{127}I$ ratios from 10^{-12} to $>10^{-9}$ [1]. Such distinct characteristics of ^{129}I sources together with the high detection sensitivity

provided by the accelerator mass spectrometer (AMS) since the 1980's has dramatically expanded the utility of ^{129}I in many fields. For example, it is now particularly applied in geological science as a unique dating tool [2-3], but also widely in environmental science as a unique and powerful tracer [4-8].

Opened in 2002, the routine measurements of the SUERC 5 MV AMS facility included ^{10}Be, ^{14}C, ^{26}Al, ^{36}Cl, ^{41}Ca and ^{129}I. Performances of ^{10}Be-, ^{14}C-, ^{26}Al- and ^{36}Cl-AMS have been previously reported [9-12]. Here, we present the performance of ^{129}I-AMS measurements made at SUERC. Although ^{129}I has no isobaric problem due to the difficulty of negative ion production of isobaric ^{129}Xe, a clear separation of any potential interfering ions by molecular fragments from the ^{129}I is important for the precise ^{129}I-AMS measurement. In normal operation of the middle-size AMS (3-5 MV), the charge state +5 seems to be the only favorable choice due to the requirement of a modest resolution and the rareness of molecular fragments [13-21]. Although the total ion transmission efficiency for $^{129}I^{3+}$ is much higher than other charge states, the $^{129}I^{3+}$-AMS has been paid much less attention yet, probably due to considerations of the same magnetic rigidity between $^{129}I^{3+}$ and the disassociated ions $^{86}Sr^{2+}$ and $^{43}Ca^{1+}$, and usually the limited bending power of the analysing magnet. However, for the natural samples with the limited amounts of iodine and low $^{129}I/^{127}I$ ratios, the high ion transmission efficiency would require routine operation of the $^{129}I^{3+}$-AMS. To obtain a full assessment on the choice of operating conditions, the subject of this study focuses on the identification of the interferences to ^{129}I-AMS, and to study the precision and accuracy of $^{129}I/^{127}I$ measurement at different charge states, the ^{129}I background level and effects of ion source cross contamination.

2. Materials and experiments

2.1. Preparation of experimental sample materials

As commonly used in other laboratories, AgI is used as the target material in this study. They include a series of diluted NIST reference (SRM4949C) with $^{129}I/^{127}I$ ratios ranging from 10^{-12} to 10^{-10} for precision and accuracy measurement of ^{129}I-AMS, and Woodward iodine with $^{129}I/^{127}I$ ratio of 3×10^{-14} [15,18] for assessment of machine ^{129}I background level. AgI is mixed with Ag (99.95 %) with a weight ratio of AgI : Ag = 1 : 2. The NEC Al target holder with 1 mm diameter is used for the ^{129}I-AMS routine operation. It should be noted that the redox reaction between AgI and Al ($3AgI + Al = 3Ag + AgI_3$) can thermodynamically occurs. However, the reaction does not take place unless there is water vapour in the environment. In our routine operation, the pressed targets were always kept dry in oven. Therefore, any drawback was not observed when using Al target holders in our study.

There are a lot of molecular fragments that might result in *E/q* and *M/q* ratios identical or close to ^{129}I, thus potentially interfering with ^{129}I determination. Figure 1 shows these ions with *E/q* and *M/q* ratios differing from $^{129}I^{n+}$ within ±2 %. In order to identify these interferences to ^{129}I-AMS, small amounts of the potential interference-containing reagent such as RhC_2 (5 % Rh), MoO_2 (99 % Mo), Te (99.99 %), $CaSO_4$, etc. are added to the Agl+Ag mixture of standard and background samples to exaggerate the potential interferences.

2.2. ^{129}I-AMS performances

Detailed description of the SUERC AMS instrument and performance can be found in [9] and the ^{129}I-AMS performance with some modifications is summarised in Table 1 and outlined as follows.

Negative ions are extracted from the sources by sputtering AgI target material with a 2.5 keV Cs^+ primary beam to protect possible melts. The extracted $^{127}I^-$ currents from ion source were adjusted below 3 μA. The negative ions with initial energy of ~62 keV were firstly selected by the 45º spherical electrostatic analyser. Subsequently, negative ions with magnetic rigidity of

8.514 will pass through the 90º injection magnet. After the injection magnet the $^{127}I^-$ ions are determined by Faraday cup at the off-axis during injection of the corresponding radioisotope $^{129}I^-$.

Table 1. Routine experimental condition of ^{129}I-AMS at SUERC

Parameter	Description
Target	AgI mixed with Ag (AgI:Ag=1:2 by weight)
Typical current	0.5-3 μA $^{127}I^-$
Cathode potential	2.5 KV
Injection energy	62 KeV
Injection mode	Sequential injection (2*ms* for $^{127}I^-$, 1*s* for $^{129}I^-$)
Stripping gas	Ar
Terminal voltage	3~3.5 MV
Particle ion transmission at 3MV	15% ($^{129}I^{3+}$), 5% ($^{129}I^{4+}$), 3% ($^{129}I^{5+}$), 1% ($^{129}I^{6+}$)
Detector window and gas	SiN (100 nm), propane
Injection magnet	Bending angle 90°, radius 45 cm, ME/q^2=15
Electrostatic spherical analyser	Bending angle 45°, radius 30 cm, E/ΔE=90
Analysing magnet	Bending angle 90°, radius 127 cm, ME/q^2=176
Electrostatic cylindrical analyser	Bending angle 20°, radius 381 cm, E/ΔE=760

The Ar gas stripper is operated at 3 MV and the following analysing magnet selects the 3+ charge states. The Ar gas stripping and transmission efficiencies are 15 % from $^{127}I^-$ to $^{127}I^{3+}$. The $^{127}I^{3+}$ ions are determined by offset Faraday cup at the exit of the analysing magnet, whereas the radionuclide $^{129}I^{3+}$ and other interferences are further analysed by electrostatic cylindrical ion energy analyser (ECA) and finally determined with the five-anode detector. The detector settings in this study include employment of a combination of SiN membrane (100 nm thickness and 10 × 10 mm width) and propane detector gas. The $^{129}I^{3+}$ and other interferences gate is set in the two dimensional E_{tot} versus dE_1 histogram.

In other high charge state (4+, 5+ and 6+) operations, most of the conditions including the injection energy, terminal voltage and detector configurations were set the same as $^{129}I^{3+}$-AMS operation. However, the analytical magnet and ECA were set to select the corresponding charge

states. In these cases, the Ar gas stripping and resulting transport efficiencies are relatively low, i.e., ~5 % $^{127}I^-$ to $^{127}I^{4+}$, ~3 % $^{127}I^-$ to $^{127}I^{5+}$ and ~1 % $^{127}I^-$ to $^{127}I^{5+}$.

3. Results and discussion

Although there are a lot of molecular fragments with *E/q* and *M/q* ratios identical or close to ^{129}I that might theoretically interfere with ^{129}I-AMS determination (Fig. 1), less interfering ions are actually observed in our routine operation. Figures 2*a-d* shows the ^{129}I-AMS spectra for the Woodward iodine, and mixtures of Woodward iodine and potential interference-containing reagents for $^{129}I^{3+}$, $^{129}I^{4+}$, $^{129}I^{5+}$ and $^{129}I^{6+}$. Note that some of the non-^{129}I signals evident in the spectra are incompletely resolved by the high energy mass spectrometer.

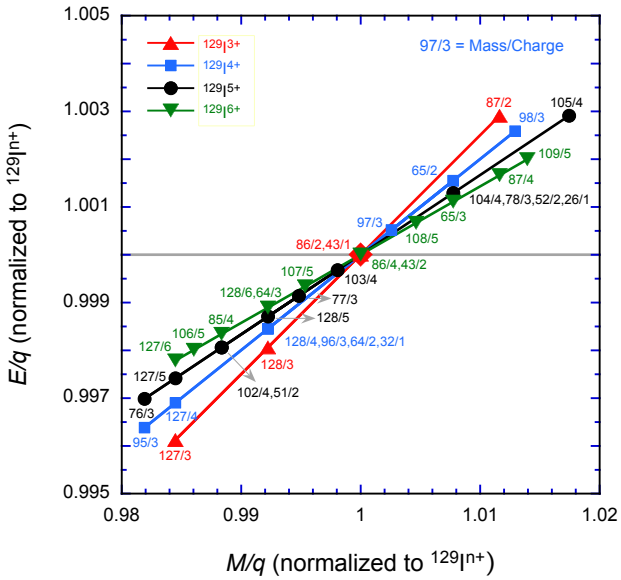

Figure 1. $^{129}I^{n+}$-normalised *E/q verse M/q* values of molecular fragments showing potential interference to $^{129}I^{n+}$ (n = 3-6).

3.1. Identification of interferences to ^{129}I

One of the most distinct features in ^{129}I-AMS spectra shown in Figs. 2*a-d* is that the $^{128}Te^{n+}$ (n = 3-6) overlap the corresponding charge states of ^{129}I peak. This can be attributed to the small difference of *M/q* and *E/q* ratios between ^{128}Te and ^{129}I. In this case, ^{128}Te ion is likely injected as $^{128}Te^1H^-$.

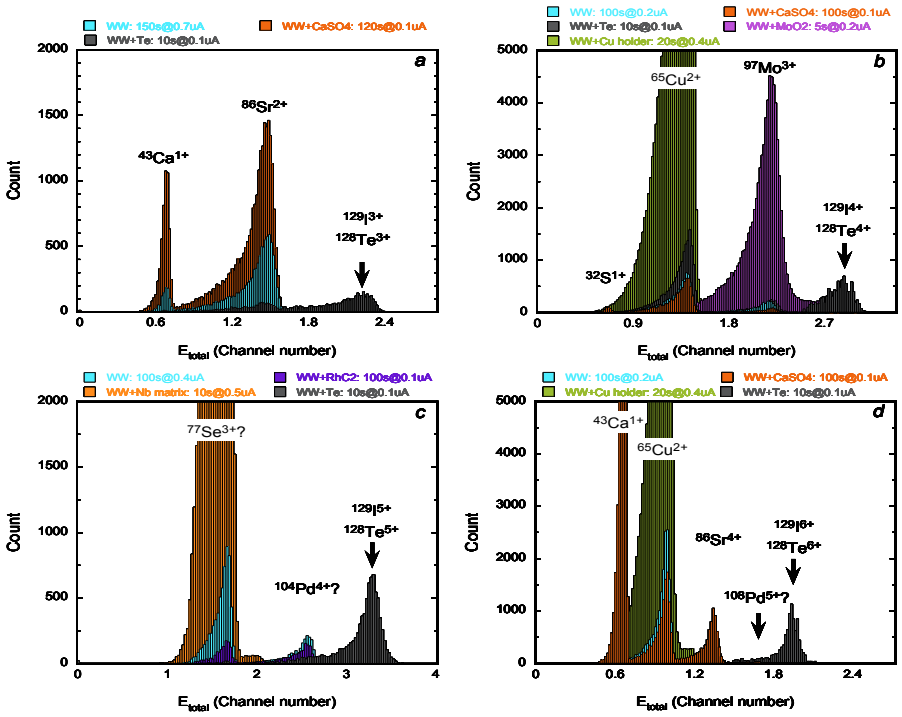

Figure 2. $^{129}I^{n+}$-AMS spectra of Woodward iodine sample (WW) and mixture of WW and potential interference-containing reagents at charge state +3 (*a*), 4+ (*b*), 5+ (*c*) and 6+ (*d*). These measurements were operated at 3 MV and employed 100 nm thickness SiN membrane and propane detector gas. Note that data for each target sample were gained in different $^{127}I^-$ current (μA) and counting time (sec.).

Figure 2*a* shows spectra of $^{129}I^{3+}$-AMS of the Woodward iodine, and mixture of Woodward iodine and chemical reagents ($CaSO_4$ and Te) at the routine condition. Two discrete peaks ($^{43}Ca^{1+}$ and $^{86}Sr^{2+}$) are close to the peak (overlapped by $^{129}I^{3+}$ and $^{128}Te^{3+}$) with 12 MeV and have relatively lower energy than $^{129}I^{3+}$ ions. These two peaks generally exist in the target samples (standard, background and unknowns). Zhao et al. have simulated the energy spectra of some hypothetical molecular fragments showing $^{43}Ca^{1+}$ and $^{86}Sr^{2+}$ ions with 1/3 and 2/3 energy of $^{129}I^{3+}$ ions, respectively [14]. Our observations are consistent with these simulations and further confirmed by adding $CaSO_4$ to the Woodward iodine samples. Regarding the injected form, in addition to $^{43}Ca^{86}Sr^-$ and $^{43}Ca_3^-$ suggested in [14], $^{43}Ca^{32}S^{18}O_3^-$ might be another candidate, as well as $^{86}Sr^{27}Al^{16}O^-$ since Al target holder is used and Sr is an inevitable impurity in Ca compounds. This is made probably more than $^{43}Ca^{32}S^{18}O_3^-$, because the spectrum with the $CaSO_4$ added gave more ^{86}Sr ions than ^{43}Ca ions.

Figure 2*b* shows $^{129}I^{4+}$ spectra of the Woodward iodine sample, mixture of Woodward iodine and potential interference-containing reagents ($CaSO_4$, MoO_2 and Te), and Woodward iodine sample pressed into Cu target holders. Three discrete peaks with lower energy are close to $^{129}I^{4+}$ and $^{128}Te^{4+}$ peaks with 15 MeV. The peak of $^{32}S^{1+}$ is identified by sputtering target samples mixed with $CaSO_4$. The $^{65}Cu^{2+}$ is identified by use of the copper sample holder. The $^{97}Mo^{3+}$ is confirmed by sputtering the target sample mixed with MoO_2. Again, these three peaks are consistent with the simulation results by Zhao et al. [14]. Although $^{32}S^{1+}$ is first demonstrated in this study implying $^{32}S^{1+}$ possible injected as $^{43}Ca^{32}S^{18}O_3^-$, the previous studies have reported existence of $^{65}Cu^{1+}$ in the $^{129}I^{2+}$ spectra [18], and $^{97}Mo^{9+}$ in $^{129}I^{12+}$ [20]. Vockenhuber et al. pointed out that $^{65}Cu^{1+}$ is likely injected as $^{63}Cu^{65}Cu^1H^-$ ions [18]. The $^{97}Mo^{16}O_2^-$ ions are commonly accepted as an injected form of $^{97}Mo^{n+}$ [13,14,16,19].

In case of $^{129}I^{5+}$-AMS (Fig. 2*c*), two discrete peaks are visible and show lower energy than $^{129}I^{5+}$ and $^{128}Te^{5+}$ peaks. According to the simulation by Zhao et al. [14] and calculations made by Kilius et al. [13] and Matsuzaki et al. [16], these two peaks would be attributed to $^{77}Se^{3+}$ and $^{103}Rh^{4+}$. Although identification of $^{77}Se^{3+}$ was not conducted with any Se-bearing reagent in this study, $^{103}Rh^{4+}$ is unlikely the interfering candidate because adding RhC_2 ($^{103}Rh^{13}C_2^-$) to the Woodward iodine sample did not elevate the peak with 2/3 energy of $^{129}I^{5+}$ ions. Honda et al. [21] observed $^{104}Pd^{4+}$ (M/q = 26) close to $^{129}I^{5+}$ (M/q = 25.8). Thus, the peak with 2/3 energy of $^{129}I^{5+}$ ion can be most likely attributed to $^{104}Pd^{4+}$. Alternatively, $^{104}Ru^{4+}$ can be considered as a potential candidate [16]. It should be noted that existence of an interference peak ($^{77}Se^{3+}$?) in the $^{129}I^{5+}$ spectra was unexpected from mixture of Woodward iodine and Nb matrix. Such interference could be attributed to impurity of Nb powder. Further studies would be necessary to clarify these alternatives and the corresponding injection forms. For example, a high energy magnet scan might further reveal whether it is $^{103}Rh^{4+}$ or $^{104}Pd^{4+}$, or both, that is the main 4+ fragment ions.

In the spectra of $^{129}I^{6+}$ (Fig. 2*d*), there are four discrete peaks close to $^{129}I^{6+}$ and $^{128}Te^{6+}$ peaks. The peaks with 1/3 and 2/3 energy of $^{129}I^{6+}$ can be attributed to $^{43}Ca^{2+}$ and $^{86}Sr^{4+}$, respectively, as shown in $^{129}I^{3+}$ spectra described above. Similar to the $^{129}I^{4+}$-AMS, the $^{65}Cu^{3+}$ peak in $^{129}I^{6+}$ spectra was confirmed by sputtering the reference sample pressed in the copper sample holder. There is no direct evidence to identify the peak with small difference of energy from $^{129}I^{6+}$ ion. As a potential candidate, $^{107}Ag^{5+}$, $^{108}Cd^{5+}$ or $^{108}Pd^{5+}$ can be considered. Kilius et al. [13] and Matsuzaki et al. [15] considered $^{111}Cd^{6+}$, which has natural relative abundance of 12.81 % Cd, as potential interference to $^{129}I^{7+}$. If this is the case, $^{108}Cd^{5+}$ with relative abundance of 0.89% Cd can be attributed to potentially interfere with $^{129}I^{6+}$ ion. At present, we do not have convincing conclusion because all $^{107}Ag^{5+}$, $^{108}Cd^{5+}$ and $^{108}Pd^{5+}$ have <1 % difference of *M/q* values from $^{129}I^{6+}$. However, on the basis of fact of $^{104}Pd^{4+}$ (11.14 % Pd) existing in $^{129}I^{5+}$-AMS [21], $^{108}Pd^{5+}$ (26.46 % Pd) would likely be an interference in addition to $^{107}Ag^{5+}$ (a main target element), both with the closest energy to $^{129}I^{6+}$. Further studies are required to clarify these alternatives, but also their corresponding injection forms.

Although M/q interferences are well resolved in the energy spectra above, it should be mentioned that pile-up might lead to interferences. We are confident that the non-^{129}I peaks are not pile-up because the event rate was low and did not affect the synthetic pulse signals used for dead-time correction.

3.2. Assessment of background ^{129}I-AMS measurement

As described above, the ^{128}Te peak overlaps the ^{129}I at each charge state, which could potentially elevate the ^{129}I background level and thus interfere the precious and accurate measurement of ^{129}I. Although there is difficulty to separate ^{129}I from ^{128}Te during the routine AMS operation, the rareness of Te in natural environmental samples and chemical reagents

fortunately makes negligible contributes to the ^{129}I-AMS detection (without using time of flight method) for samples after careful chemical preparation.

It has been discussed that different types of matrix and sample holder can elevate the background level of ^{129}I-AMS [18,19]. To investigate if this is a case at SUERC AMS, an assessment of ^{129}I background has been conducted by use of different types of matrix (*Ag versus Nb*) and sample holders (*Al versus Cu*). It was found that there is no significant difference on ^{129}I/^{127}I ratio between Ag and Nb powder matrix in most cases. However, the Nb powder matrix can potentially elevate $^{129}I^{5+}$ background because it can produce exceeding amounts of $^{77}Se^{3+}$ ions which might subsequently cause ion scattering in the detector (Fig. 2*c*). Similarly, the copper sample holder can potentially elevate $^{129}I^{4+}$ and $^{129}I^{6+}$ background by contributing exceeding amounts of $^{65}Cu^{2+}$ ions in $^{129}I^{4+}$-AMS and $^{65}Cu^{4+}$ in $^{129}I^{6+}$-AMS (Figs. 2*b,d*). The severity of these background ions would be system dependent as these background ions do have different E/q and M/q values from those of ^{129}I.

Due to the volatility of iodine, ion source memory might be a significant issue of high ^{129}I background as observed in other AMS laboratories [18]. Like ^{36}Cl-AMS at SUERC, such cross contamination can be effectively reduced by the use of modified immersion lenses [11]. As shown in Fig. 3, after long-time measurements of the high-level samples (^{129}I/^{127}I of 10^{-11}), the measured ^{129}I/^{127}I in the low-level Woodward iodine carrier elevated and then declined exponentially. This suggests that care should be taken to properly arrange the sample order/group in order to measure from low to high ratio and/or give enough pre-sputtering times during the ^{129}I-AMS measurement. Even though work is still ongoing to reduce our source memory, the current performance is completely acceptable due to our measurement sequencing algorithm that minimises the effect. The repeated Woodward iodine measurements indicate that the background level of ^{129}I-AMS system at SUERC is fairly low (^{129}I/^{127}I of ~10^{-14}). Therefore, in our routine analysis, any correction for source memory is not applied.

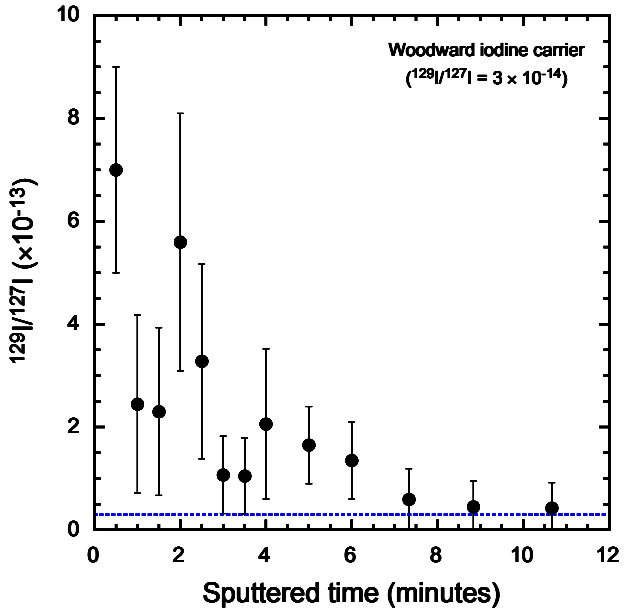

Figure 3. Temporal variation of $^{129}I/^{127}I$ ratios of low-level Woodward sample measured after sputtering (~1 *h*) on a standard with $^{129}I/^{127}I = 1.047 \times 10^{-11}$.

3.3. Precision and accuracy of $^{129}I^{3+}$-AMS measurement

A series of ^{129}l reference samples with ^{129}l/^{127}l nominal ratios ranging from 10^{-12} to 10^{-10} (*n* = 6) have been measured for investigations of precision and linearity. In our routine ^{129}I-AMS analysis, the normalization factor generally varies from 1.2 to 1.4. The good consistence between the measured and nominal values suggest fair linearity (R^2 = 1, not shown) and precision of ^{129}I-AMS measurements at SUERC. Overall, the reference samples have standard deviations of 3 % with average 3 % difference from the nominal values, indicating that the $^{129}I/^{127}I$ ratio is being performed routinely at the precision and accuracy of ~3 % at >10^{-12} level at SUERC. As an example, Figure 4 shows probability plots of $^{129}I/^{127}I$ ratios measured on a secondary reference standard during the period of 2012-2016. This secondary standard has nominal $^{129}I/^{127}I$ ratio of 1.047×10^{-11}, which was also diluted from NIST SRM4949C as prepared for the primary standard with $^{129}I/^{127}I = 1.089 \times 10^{-10}$. The $^{129}I/^{127}I$ ratio of the secondary standard is similar to the range of typical unknown samples. The probability plots reveal that measurement mean and standard deviation of $^{129}I/^{127}I$ ratio are 1.049×10^{-11} and 2.62

$\times 10^{-13}$, respectively, which results in a 2.5 % scatter. The mean propagated 1σ relative measurement uncertainty (the error bars) is 3 %. The data sets are well described by the plotted Gaussian curves, with fits shown (Fig. 4).

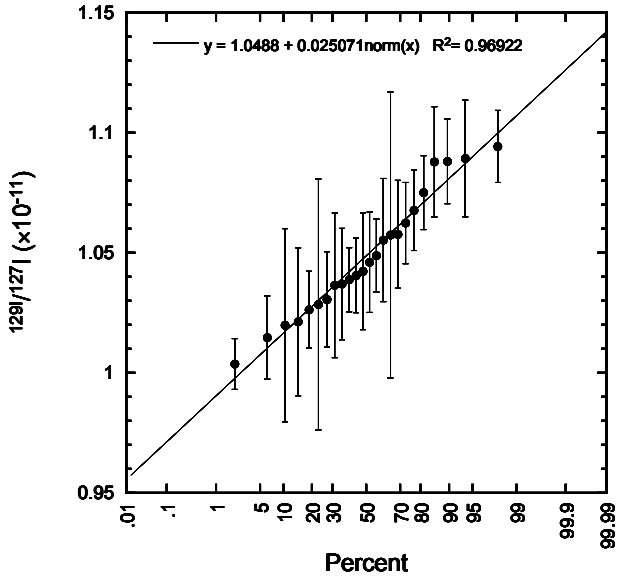

Figure 4. Probability plot of the long-term $^{129}I/^{127}I$ measurements of the secondary standard sample with $^{129}I/^{127}I$ of 1.047×10^{-11}, normalized to the primary standard with $^{129}I/^{127}I$ of 1.089×10^{-10}, both of which were diluted from NIST reference (SRM4949C).

4. Conclusions

Several interferences to ^{129}I have been found during the ^{129}I-AMS measurements at charge state 3+, 4+, 5+ and 6+. These include $^{43}Ca^{1+}$ and $^{86}Sr^{2+}$ to $^{129}I^{3+}$; $^{32}S^{1+}$, $^{65}Cu^{2+}$ and $^{97}Mo^{3+}$ to $^{129}I^{4+}$; $^{77}Se^{3+}$ and $^{104}Pd^{4+}$ (or $^{104}Ru^{4+}$) to $^{129}I^{5+}$; $^{43}Ca^{2+}$, $^{65}Cu^{3+}$, $^{86}Sr^{4+}$ and $^{108}Pd^{5+}$ (or $^{107}Ag^{5+}$ and $^{108}Cd^{5+}$) to $^{129}I^{6+}$, in addition to common ^{128}Te interfering to ^{129}I in all charge states. The rareness of Te in natural environmental samples and chemical reagents makes its contribution negligible to the ^{129}I detection for samples after careful chemical preparation. Like other AMS laboratories, the $^{129}I^{5+}$ is routinely conducted for environmental level samples at SUERC whereas the $^{129}I^{3+}$ is chosen for $^{129}I/^{127}I$ analysis of natural level samples. In both cases, the precision and accuracy of $^{129}I/^{127}I$ ratio measurement are 3 % at $^{129}I/^{127}I \sim 10^{-12}$ level. The background of $^{129}I/^{127}I$ is in the range of 10^{-14}. About 1,000 measurements of ^{129}I-AMS have

been conducted since the establishment of the SUERC AMS facility. This mainly includes applications of anthropogenic ^{129}I as an environmental tracer [22,23].

Acknowledgements

We are grateful to X.L. Hou of Technical University of Denmark for his kind help in iodine chemistry and SUERC AMS colleagues for their help in ^{129}I-AMS operations. We would like to thank two reviewers for their thorough reviews, which greatly helped to improve the original manuscript.

References

[1] M.J.M. Wagner, B. Dittrich-Hannen, H.-A. Synal, M. Suter, U. Schotterer, Nucl. Instr. Meth. B 113 (1996) 490–494.

[2] U. Fehn, J.E. Moran, G.T. Snyder, Y. Muramatsu, Nucl. Instr. Meth. Phys. Res. B 259 (2007) 496–502.

[3] T. Jabbar, P. Steier, G. Wallner, O. Cichocki, J.H. Sterba, J. Environ. Radioact. 120 (2013) 33–38.

[4] M. Paul, D. Fink, G. Hollos, A. Kaufman, W. Kutschera, M. Magaritz, Nucl. Instr. Meth. Phys. Res. B 29 (1987) 341-345.

[5] G.M. Raisbeck, F. Yiou, Z.Q. Zhou, L.R. Kilius, J. Mar. Syst. 6 (1995) 561-570.

[6] J.N. Smith, F.A. McLaughlin, W.M. Smethie, S.B. Moran, K. Lepore, J. Geophys. Res. 116 (2011) C04024.

[7] R. Michel, A. Daraoui, M. Gorny, D. Jakob, R. Sachse, L. Tosch, H. Nies, I. Goroncy, J. Herrmann, H.-A. Synal, M. Stocker, V. Alfimov, Sci. Total Environ. 419 (2012) 151-169.

[8] Y. Muramatsu, H. Matsuzaki, C. Toyama, T. Ohno, J. Environ. Radioact. 139 (2015) 344-350.

[9] C. Maden, P. Anastas, A. Dougans, S. Freeman, R. Kitchen, G. Klody, C. Schnabel, M. Sundquist, K. Vanner, S. Xu, Nucl. Instr. Meth. B 259 (2007) 131–139.

[10] S. Xu, A. Dougans A., S. Freeman, C. Schnabel, K. Wilcken, Nucl. Instr. Meth. B 268 (2010) 736–738.

[11] S. Xu, S. Freeman, D. Rood, R. Shanks, Nucl. Instr. Meth. B 333 (2014) 42–45.

[12] K. Wilcken, S. Freeman, A. Dougans, S. Xu, R. Loger, C. Schnabel, Nucl. Instr. Meth. B 268 (2010) 748–751.

[13] L.R. Kilius, X.-L. Zhao, A.E. Litherland, K.H. Purser, Nucl. Instr. Meth. B 123 (1997) 10–17.

[14] X.-L. Zhao, A.E. Litherland, W.E. Kieser, C. Soto, Nucl. Instr. Meth. B 259 (2007) 265–270.

[15] H. Matsuzaki, Y. Muramatsu, K. Kato, M. Yasumoto, C. Nakano, Nucl. Instr. Meth. B 259 (2007) 721–726.

[16] H. Matsuzaki, C. Nakano, Y. Tsuchiya, S. Ito, A. Morita, H. Kusuno, Y. Miyake, M. Honda, A.T. Bautista VII, M. Kawamoto, Nucl. Instr. Meth. B 361 (2015) 63–68.

[17] N. Buraglio, A. Aldahan, G. Possnert, Nucl. Instr. Meth. B 161-163 (2000) 240–244.

[18] C. Vockenhuber, N. Casacuberta, M. Christl, H.-A. Synal, Nucl. Instr. Meth. B 361 (2015) 445–449.

[19] P. Sharma, D. Elmore, T., Miller, S. Vogt, Nucl. Instr. Meth. B 123 (1997) 347–351.

[20] Y. Nagashima, R. Seki, K. Sasa, T. matsuhiro, T. Takahashi, Y. Tosaki, K., Bessho, H. Matsuuma, T. Miura, Nucl. Instr. Meth. B 259 (2007) 241–245.

[21] M. Honda, Y. Takaku, H. Matsuzaki, A. Sakaguchi, K. Sueki, Nucl. Instr. Meth. B (this volume).

[22] C. Schnabel, V. Olive, M. Atarashi-Andoh, A. Dougans, R. Ellam, S. Freeman, C. Maden, M. Stocker, H.A. Synal, L. Wacker, S. Xu, Appl. Geochem. 22 (2007) 619–627.

[23] S. Xu, S. Freeman, X.L. Hou, A. Watanabe, K. Yamaguchi, L.Y. Zhang, Environ. Sci. Tech. 47 (2013) 10851–10859.